Automated Analysis of Collagen Histology in Ageing Skin

Osman S. Osman[1,2], Joanne L. Selway[1], Parvathy E. Harikumar[1],
Sabah Jassim[2] and Kenneth Langlands[1]

[1]*The Clore Laboratory, University of Buckingham, Hunter Street, Buckingham U.K.*
[2]*Department of Applied Computing, University of Buckingham, Hunter Street, Buckingham U.K.*

Keywords: Skin, Dermis, Collagen, Image Analysis, Histology, Unsupervised, Picrosirius, Herovici, Fast Fourier Transform, K-Means Clustering, Ageing, Aging.

Abstract: Traditionally, expert analysis is required to evaluate pathological changes manifested in tissue biopsies. This is a highly-skilled process, notwithstanding issues of limited throughput and inter-operator variability, thus the application of image analysis algorithms to this domain may drive innovation in disease diagnostics. There are a number of problems facing the development of objective, unsupervised methods in morphometry that must be overcome. In the first instance, we decided to focus on one aspect of skin histopathology, that of collagen structure, as changes in collagen organisation have myriad pathological sequelae, including delayed wound healing and fibrosis. Methods to quantify incremental loss in structure are desirable, particularly as subclinical changes may be difficult to assess using existing criteria. For example, collagen structure is known to change with age, and through the calculation of foci distances in ellipses derived from the Fourier scatter, we were able to measure a decrease in collagen bundle thickness in picrosirius stained skin with age. Another key indicator of skin physiology is new collagen synthesis, which is necessary to maintain a healthy integument. To investigate this phenomenon, we developed a colour-based image segmentation method to discriminate newly-synthesised from established collagen revealed by Herovici's polychrome staining. Our scheme is adaptive to variations in hue and intensity, and our use of K-means clustering and intensity-based colour filtering informed the segmentation and quantification of red (indicating old fibres) and blue pixels (indicating new fibres). This allowed the determination of the ratio of young to mature collagen fibres in the dermis, revealing an age-related reduction in new collagen synthesis. These automated colour and frequency domain methods are tractable to high-throughput analysis and are independent of operator variability.

1 INTRODUCTION

Analysis of tissue biopsies by histopathological methods provides the cornerstone of clinical diagnosis, although the rigorous assessment of any pathological features relies upon the experience of at least one expert pathologist. The automated classification of histological images would alleviate the burden on health care services, and provide unbiased and quantitative measurements to assist in disease identification and prognostication.

Our group has a particular interest in diseases of the skin, which are debilitating and their management has huge financial implications. By developing methods to allow morphometric analysis of tissue samples, we hope to shed new light on the pathophysiological processes underlying a range of common disorders. In particular, we have chosen to focus on the dermis and its rich collagen network, changes in which are associated with effects such as scarring, delayed wound healing and a loss of skin integrity. Rather than a simple collagenous pad, the dermis is composed of a highly-organised extracellular matrix (ECM) of proteins and other macromolecules, assembled into a meshwork of primarily collagen fibres (McGibbon, 2006). Traditionally, evaluation of this compartment was made using electron microscopy (EM), which requires both expensive equipment and extensive tissue preparation, thus this analysis tends to be research-focused. Our approach is to exploit methods available to routine histopathology laboratories, thereby broadening their utility.

In pathological states, or in ageing, the structure of collagen in the skin diverges from a regular 'basket-weave', in which collagen fibres intersect at

approximately 90° angles (van Zuijlen et al., 2003, Rawlins et al., 2006), and the production of new collagen may be perturbed (Varani et al., 2000, Mays et al., 1991, Varani et al., 2006). The latter may also be associated with dermal attrition (Al-Habian, 2011). A range of histological stains are used to identify collagens in tissue specimens, and one may make qualitative assessments of ECM integrity from photomicrographs. We and others have developed methods to quantify collagen bundle thickness and orientation, although a degree of user intervention is required with some methods (Noorlander et al., 2002), and wholly unsupervised (thus unbiased) image analysis methods, as we have previously described, are preferable (Osman et al., 2013). Moreover, in our experience variation in staining characteristics across specimens presents considerable technical difficulties that are exacerbated if tissues prepared by multiple laboratories are to be analysed.

Methods that exploit frequency domain transformations to measure fibre size have been attempted (Verhaegen et al., 2012), although no method has been developed to date that can provide user-independent analysis (Menesatti et al., 2012). We sought to improve upon existing methods in several ways: firstly by improving pre-processing to ensure uniformity between images and reduce artefacts; secondly, we used cross-polar images of picrosirius stained sections, rather than simple H&E images, as these reveal the regular collagen matrix structure rather than the loops and whirls revealed with other techniques; and thirdly we used an ellipse approximation of the fast Fourier transform (FFT) spectrum scatter rather than gravity centres as used previously (Verhaegen et al., 2012). This latter stage allows for the inclusion of more data-points in the scatter, and this is especially useful when younger skin is analysed.

In addition to the use of frequency domain analysis to establish collagen fibre size, we also wanted to adapt colour segmentation methods to allow the assessment of collagen dynamics. Herovici's polychrome is a particularly effective connective tissue stain in that it discriminates young from old collagen fibres. While this is, in principle, a simple image analysis problem based around the separation of two distinct hues, we found that variation between images made it impossible to achieve accurate quantification of red (mature collagen) and blue (young collagen) staining areas consistently. To resolve this, we implemented a dynamic approach to improve colour segmentation by exploiting K-means clustering.

Herein, we describe the development of automated methods that utilise either the frequency domain or colour space in order to assess collagen bundle thickness and collagen dynamics respectively, from images of skin sections stained with histological dyes. These tools enabled us to investigate the effects of chronological ageing on collagen structure and synthesis in an animal model of skin ageing.

2 BIOLOGICAL METHODS

2.1 Animal Models

All procedures were conducted in accordance with the UK Government Animals (Scientific Procedures) Act 1986, and approved by the University of Buckingham Ethical Review Board. C57Bl6 mice were maintained on chow diets fed *ad libitum* under standard conditions (BeeKay Number 1, B&K Universal Ltd, Leeds, UK). Mice were obtained from Charles River (Manston, UK) aged 5-6wk. Wild-type C57 mice were killed at 3mth, 8mth, 12mth and 20mth of age. Freely-fed males were used for all studies, and tissues from at least 3 animals per group were studied.

2.2 Tissue

Once animals were euthanized, dorsal skin biopsies were taken immediately and snap frozen in liquid nitrogen prior to storage at -80°C until all samples were ready for simultaneous processing to minimise artefacts. Samples were transferred to cold (4°C) 10% neutral buffered formalin then fixed for 7-8h at room temperature. This was followed by dehydration, clearing and wax immersion in an automated tissue processor as standard. Rectangular pieces of skin were placed on their sides in moulds such that sections were cut orthogonal to the epidermal surface, before embedding in paraffin wax. 4μm thick sections were cut using a rotary microtome with a knife angle of 35° and a clearance angle between 1° and 5°, before transfer to positively-charged glass slides. Haematoxylin and Eosin (H&E) staining was carried out as standard to confirm tissue integrity and orientation in all samples.

2.3 Histological Staining

Standard morphology was assessed with H&E stained images captured in bright-field with an

Aperio whole-slide scanner (Aperio, Vista, CA, USA). The depth of the dermis was measured in Aperio ImageScope software (version 11.1.2.760) using the ruler function. Dermal depth was measured from the basement membrane (epidermal-dermal junction) to the adipocyte-dermis junction. The orientation of the measurement was dictated by the basement membrane, and this followed the contour of the epidermis. At least 3 animals per group were studied, and from each animal least 3 images were captured. A minimum of 5 depth measurements were taken for each image.

Collagen organisation was studied by picrosirius staining, performed as previously described (Junqueira et al., 1979, Osman et al., 2013). Images were captured at 90x magnification from at least 3 discrete locations per slide with a Nikon TEi inverted microscope equipped with cross-polar optics and a QImaging CCD camera (all supplied by Nikon, Kingston, UK) coupled to Nikon NIS Elements software (version 4.10.01). Collagen dynamics were evaluated from whole-slide bright-field captures of Herovici's polychrome staining (Friend, 1963, Cook, 1974). Standardised regions of interest (ROIs) showing papillary dermis (inclusive of the basement membrane, but excluding non-dermal tissues such as hair follicles) where captured using a 40x objective lens.

2.4 Statistical Analysis

Data analysis was performed using GraphPad Prism 5.0. One-way ANOVAs compared collagen patterns in 3mth controls (by which age rates of collagen synthesis are stable) (Taher et al., 2011, Yano et al., 2001, Muller-Rover et al., 2001) to test groups. Dunnett's post-hoc analysis was performed where the ANOVA demonstrated significance. Where appropriate, Pearson's correlation analysis was performed ($p < 0.05$). For all tests: * $p < 0.05$; ** $p < 0.01$; *** $p < 0.001$; **** $p < 0.0001$.

3 COMPUTATIONAL METHODS

3.1 Measurement of Collagen Bundle Thickness and Spacing

All image processing and analysis was performed in MATLAB (R2011b, MathWorks, Cambridge, UK) equipped with the Image Processing Toolbox. Images were pre-processed with an unsharp filter to enhance edges (in various orientations) and other high-frequency components (Humaimi et al., 2001,

Cheikh and Gabbouj, 1998). Specifically, the unsharp filter was applied the the greyscale conversion of the original picrosirius stained image to create a mask. This mask was then subtracted from the original greyscale image to produce a sharper image with clear collagen edges. An usharp mask filter was applied according to the formula (1):

$$G(x, y) = f(x, y) - fsmooth(x, y) \qquad (1)$$

where fsmooth(x,y) is the smooth version of original image f(x,y).

The resulting sharpened image was produced by formula (2):

$$Fsharp(x, y) = f(x, y) + k \cdot G(x, y) \qquad (2)$$

where k is a scaling constant between 0.2 and 0.7

Each image was then converted to greyscale and the discrete Fourier transform (DFT) was computed with the Fast Fourier Transformation (FFT) function in MATLAB. The FFT is an efficient algorithm that returns the strength of the different frequency waveforms contributing to the pixel values of the entire image (Blanchet and Charbit, 2010).

The texture of the Fourier spectrum was used to determine the relative organisation or directionality of the original image texture. Power spectral analysis of an image can be interpreted as an averaging of the FFT spectrum at different frequency sub-bands.

The highest frequency range sub-band of the FFT was exploited to generate a power plot of the FFT spectrum (Figure 1 and 3), this computed by calculating the higher frequencies using the MATLAB code in formula (3):

$$\begin{aligned} FFTmax \\ = max\left(max\left(log\left(abs\left(FFT2(image)\right)\right)\right)\right) \end{aligned} \qquad (3)$$

The resulting spectra were transformed into binary through Otsu thresholding (Figure 1 and 3), and elliptical measurements of the scatter pattern for each spectrum were made. Briefly, the ellipse with the same normalized second central moment as the segmented binarised scatter was generated. The variance in the region was calculated using a MATLAB function (regionprops) to find the major and minor axes of the fitted ellipse.

From the elliptical scatter, measurements of average collagen bundle thickness were extracted using the location of the foci of ellipses, and the distances between the foci and the verteces of the ellipses (Figure 1 and 3). Measurements of the axes of the ellipses were not defined by spatial position, but defined by the variance of the region. Formulas (4) and (5) define this process:

$$\overline{F = \sqrt{(A^2 - B^2)}} \qquad (4)$$

$$T = A - F \qquad (5)$$

where T is the distance between foci and the verteces of any ellipse (representing bundle thickness), F is the distance in μm from each focus to the centre and A and B are the major and minor radii of the ellipse in μm. This process is summarised in Figure 1. Typical FFT scatter patterns and ellipses derived from an ageing mouse skin model are shown in Figure 3.

3.2 Measurement of Collagen Dynamics

Image segmentation based on red, green and blue (RGB) pixel colour values informs the separation of objects within a given colour space (Menesatti et al., 2012, Hosea et al., 2011), allowing areas with similar values to be quantified as one entity. Although not universally exploited in biomedical imaging, RGB-based segmentation is commonly used in morphometry and we used this approach herein. Specfically, we sought to develop colour filter-based segmentation of Herovici stained skin images towards the quantification of both newly-synthesised and mature collagen.

Our approach involved the determination of pixel intensity values for each of the red, green and blue channels in the Herovici RGB image. This was followed by segmentation of red and blue pixels using two steps: reducing the multiplicity of colours in the image and selecting all red (and "reddish") pixels, as well as all blue (and "bluish") pixels, followed by colour segmentation using discrete criteria to segment all the pixels accurately.

Using this thresholding technique, we initially applied a simple segmentation algorithm to a region of interest (ROI) within the upper (papillary) dermis to quantify red and blue fibres according to the following formulae (6), (7) and (8).

Red if:

$$Value\ of\ R > (G+B) \cdot C1; \qquad (6)$$

Blue if:

$$Value\ of\ B > (G+R) \cdot C2; \qquad (7)$$

$$Pixel = 255\ if\ not\ blue\ or\ red \qquad (8)$$

where R, G, and B are Red, Green and Blue respectively, C1=0.75 and C2=0.9 (determined empirically for each image set).

Due to the inherent variability in staining properties between histological samples, our initial attempts to simply segment the red and blue pixels
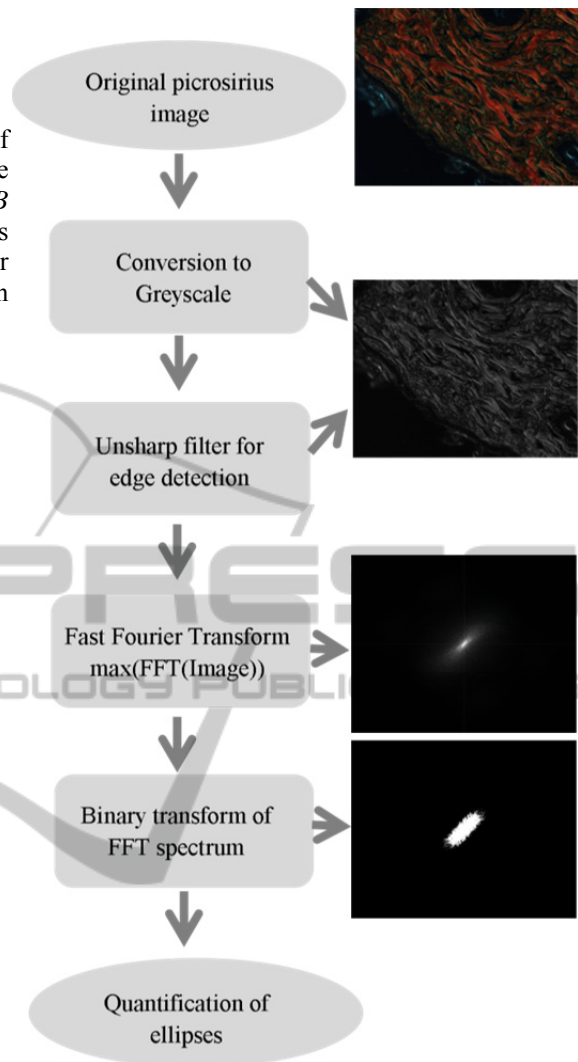

Figure 1: Flow chart for the measurement of collagen bundle thickness in picrosirius images.

using standard thresholds according equations 5 and 6 were unsatisfactory (Figure 4C and 4D). In order to improve this, we employed an iterative K-means clustering method to refine pixel intensity values derived from a range of images to allow more accurate segmentation (Yerpude and Dubey, 2012, Farivar et al., 2008).

This method is described in the flow chart in Figure 2. Briefly, for each image a median 3x3 filter was applied to the image to remove noise, then contrast stretching was performed using the MATLAB function "*imadjust*" (this acts to increase the dynamic range of an image such that 1% of all pixel values are saturated at low and high intensities of the image). Subsequently, RGB images were

converted into CIE L*a*b* colour space, and K-means clustering was performed to partition the data points into three clusters. The centroids of the clusters were computed and their associated Voroni diagram was constructed. The data points were then assigned to the cluster with the closest centroid measured by Euclidian Distance. Once allocated, centroids were recalculated, and the clustering process was repeated until the groups stabilised (Yerpude and Dubey, 2012, Farivar et al., 2008). This process was followed by segmentation and image histogram-based thresholding to remove bright pixels from segmented images.

4 APPLICATION OF METHODS

4.1 Quantification of Collagen Changes in Chronologically-aged Skin

We subjected replicate images derived from a model of skin ageing to quantitative analysis. We and others previously showed that both collagen organisation and dynamics are compromised with increasing age (Varani et al., 2006, Osman et al., 2013). We initially attempted to use existing methods to measure collagen bundle thickness using gravity centres isolated from the FFT scatter created from images of H&E stained skin (Verhaegen et al., 2012). However, we found that we could not replicate this analysis without significant user interaction, for example in mapping gravity centres. Moreover, as picrosirius images more effectively reveal collagen structure, we wished to investigate the possibility that the analysis of these images would overcome problems associated with the analysis of H&E images. Our approach is summarised in Figure 2 and Figure 4.

Our measurements revealed a correlation with chronological ageing and reduction in fibre thickness (Figure 4D). Not only were we able to quantify gross changes associated with extremes of age (i.e. between 3mth [the equivalent of young adulthood] and 20mth [equivalent to extreme old age in humans]), we were also able to resolve incremental reductions in collagen bundle thickness over shorter time-spans, with a significant negative correlation observed between chronological age and bundle size (r^2=0.8268, p<0.05).

Rodent hair follicle cycling is synchronous in the first few weeks post-partum, which is important as collagen synthesis is coordinated with the growth, resting and regenerative stages of the hair follicle cycle (Taher et al., 2011, Yano et al., 2001,
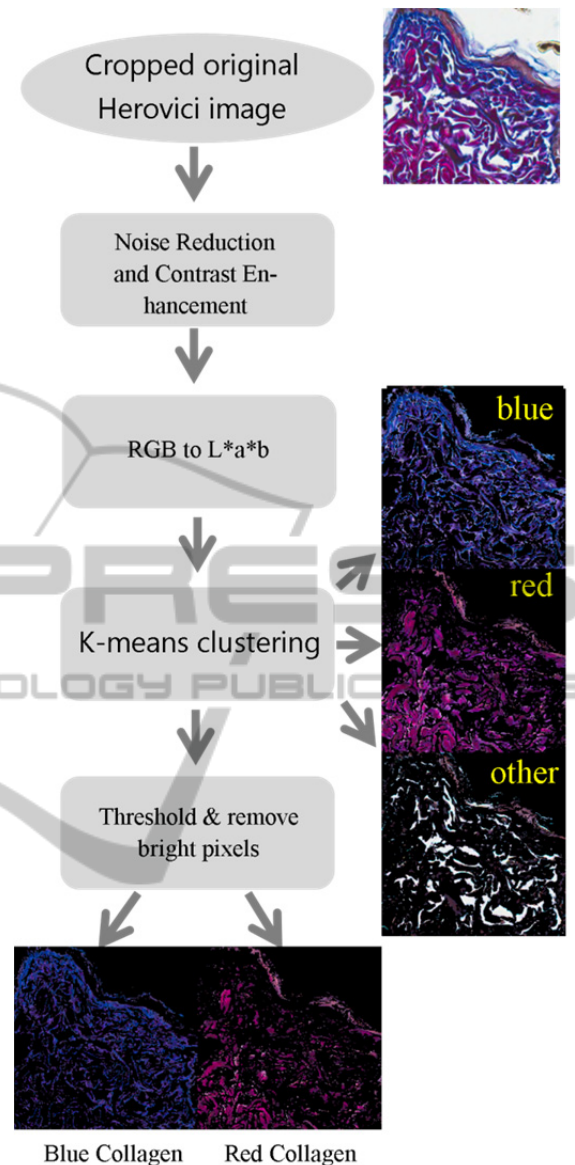

Figure 2: Flow diagram of our K-means clustering based method for the quantification of young (blue) and mature (red) pixels in images of Herovici stained skin.

Rodent hair follicle cycling is synchronous in the first few weeks post-partum, which is important as collagen synthesis is coordinated with the growth, resting and regenerative stages of the hair follicle cycle (Taher et al., 2011, Yano et al., 2001, Muller-Rover et al., 2001). For this reason, we analysed an expanded panel of skin samples by Herovici's polychrome stain to investigate collagen dynamics (Figure 4). If simple segmentation methods were used (i.e. without a clustering step to optimise colour values used to inform segmentation), then no correlation could be established between collagen

synthesis and age (3 to 20mth inclusive; $r^2=0.8723$, $p>0.05$) due to the influence of inter-image variation (Figure 4C and 4D). Conversely, the use of K-means clustering to inform our quantification method did reveal a correlation between a decrease in newly-synthesised collagen relative to mature collagen and time (between 3 and 20mth inclusive, $r^2=0.9438$, $p<0.05$; Figure 4E and 4F). The relative reduction in new collagen synthesis observed in skin taken from 7 week old mice is most likely as a consequence of the establishment of the adult dermis at this phase of the mouse life cycle. After this time hair follicle cycling becomes asynchronous, and collagen synthesis stabilises.

5 CONCLUSIONS

Murine models of human disease are widely used by the biomedical science community, and these include studies of the skin. A loss of skin structure is associated with a loss of function, and damage to the dermal layers is seen in chronological ageing, in response to environmental challenges such as sun exposure, or in diseases such as diabetes. Objective measurements of dermal structure following therapeutic intervention (made by assessing collagen integrity) would facilitate the evaluation of agents effective in treating, for example, impaired wound healing. Ideally, such analysis be completely unsupervised and tractable to high-throughput studies. However, one of the major obstacles to the effective automation of morphometry is in handling the variation in colour intensity and hue displayed between images, even when every effort is made to reduce such technical variation. In order to address this, we have developed robust techniques to determine collagen structure and dynamics in histological preparations of mammalian skin. By exploiting information in the frequency domain, and by using a K-means clustering algorithm to stabilise inter-image variation, we were able to quantify subtle changes in structure in a model of ageing. Further investigation of a wider range of biological samples is required to ensure that these algorithms are truely data-set independent, and we are in the process of applying our methods to the annotation of skin images generated by a high-throughput phenotyping study. Such an undertaking would not be possible if each image had to be assessed independently and subjected to manual semi-quantitative analysis.

We are confident that our methods are adaptable to the quantification of pathological features in human skin biopsies, and may eventually lead to the creation of quantitative tools for pathologists and basic researchers.
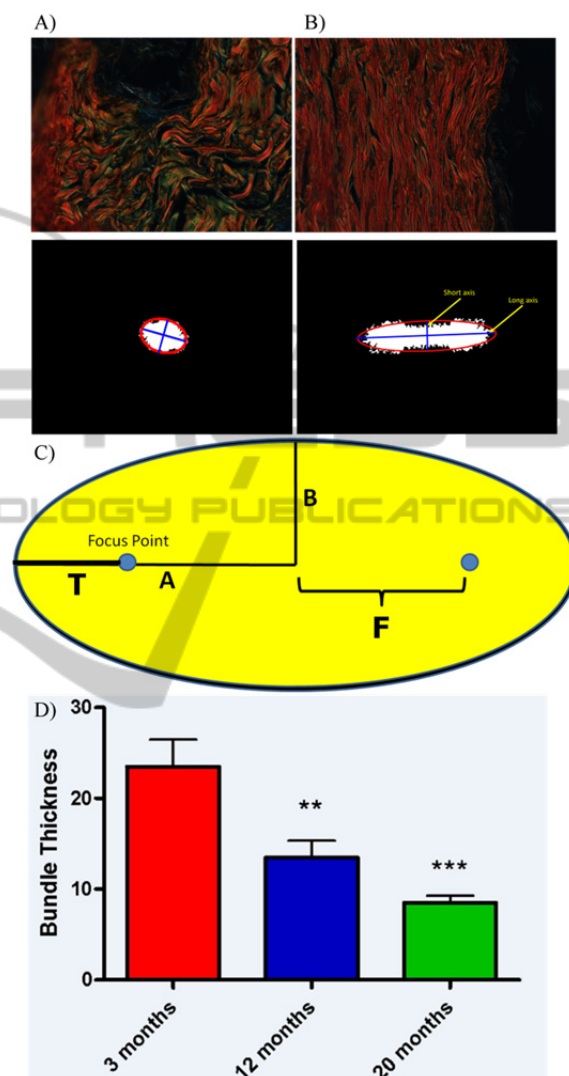

Figure 3: Measurement of collagen bundle thickness. Representative cross-polar images of picrosirius stained mouse skin A) 3mth and B) 20mth and corresponding binarised FFT scatter with fitted ellipses and axes superimposed. Images were captured at 90x original magnification. C) Diagram explaining the generation of ellipse parameters. D) Decrease in collagen bundle thickness in an ageing skin series.
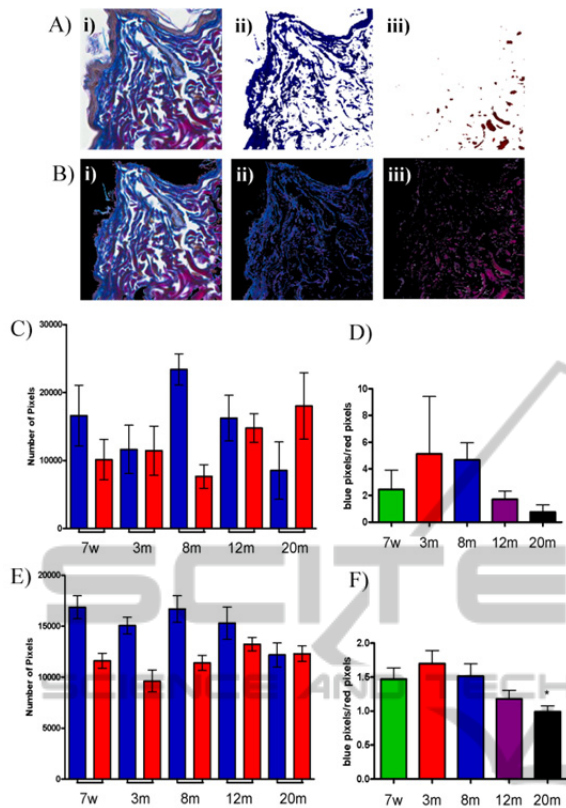
Figure 4: Quantification of collagen dynamics. Ai) Typical original ROI from Herovici stained mouse skin (3mth; 90x original magnification), ii) segmentation using blue criteria, iii) segmentation using red criteria. Bi) Image ready for K-means-informed segmentation (after removal of background and epidermis by thresholding the saturation channel of HSV colour space), ii) blue cluster pixel segmentation, iii) red cluster pixel segmentation. C) Pixel values obtained by simple blue and red segmentation or by the K-means clustering method (E) in the ageing series. D) and F) The ratio of blue to red pixels in images achieved by either simple segmentation D) or K-means clustering (F).

ACKNOWLEDGEMENTS

REFERENCES

Al-Habian, A. Z., M. S.; Stocker, C. J.; Kepczynska, M. A.; Wargent, E. T.; Cawthorne, M. A.; Langlands, K 2011. Abstract: Increasing insulin resistance correlates with progressive skin damage in murine models of obesity and diabetes. *Journal of Investigative Dermatology,* 131**,** S34.

Blanchet, G. & Charbit, M. 2010. *Digital Signal and Image Processing Using MATLAB*, Wiley.

Cheikh, F. & Gabbouj, M. 1998. Directional Unsharp Masking-Based Approach for Color Image Enhancement. *In:* Marshall, S., Harvey, N. & Shah, D. (eds.) *Noblesse Workshop on Non-Linear Model Based Image Analysis.* Springer London.

Cook, H. C. 1974. *Manual of histological demonstration techniques,* Boston, Butterworths.

Farivar, R., Rebolledo, D., Chan, E. & Campbell, R. Year. A parallel implementation of k-means clustering on GPUs. *In:* Proceedings of International Conference on Parallel and Distributed Processing Techniques and Applications (PDPTA), 2008. 340-345.

Friend, W. G. 1963. A polychrome stain for differentiating precollagen from collagen. *Stain Technology,* 38**,** 204-206.

Hosea, S. P., Ranichandra, S. & Rajagopal, T. 2011. Color Image Segmentation–An Approach. *Color Image Segmentation–An Approach,* 2.

Humaimi, M. N., Razif, M. R. M. & Nagoor, M. T. A. 2001. Comparison between Median, Unsharp and Wiener filter and its effect on ultrasound stomach tissue image segmentation for Pyloric Stenosis. *International Journal of Applied Science and Technology,* 1**,** 218-226.

Junqueira, L. C., Bignolas, G. & Brentani, R. R. 1979. Picrosirius staining plus polarization microscopy, a specific method for collagen detection in tissue sections. *Histochem J,* 11**,** 447-455.

Mays, P. K., Mcanulty, R. J., Campa, J. S. & LAURENT, G. J. 1991. Age-related changes in collagen synthesis and degradation in rat tissues. Importance of degradation of newly synthesized collagen in regulating collagen production. *Biochem J,* 276 (Pt 2)**,** 307-313.

Mcgibbon, D. 2006. Rook's Textbook of Dermatology, 7th edition. *Clinical and Experimental Dermatology,* 31**,** 178-179.

Menesatti, P., Angelini, C., Pallottino, F., Antonucci, F., Aguzzi, J. & Costa, C. 2012. RGB color calibration for quantitative image analysis: the "3D thin-plate spline" warping approach. *Sensors (Basel),* 12**,** 7063-7079.

Muller-Rover, S., Handjiski, B., Van Der Veen, C., Eichmuller, S., Foitzik, K., Mckay, I. A., Stenn, K. S. & Paus, R. 2001. A comprehensive guide for the accurate classification of murine hair follicles in distinct hair cycle stages. *J Invest Dermatol,* 117**,** 3-15.

Noorlander, M. L., Melis, P., Jonker, A. & Van Noorden, C. J. 2002. A quantitative method to determine the orientation of collagen fibers in the dermis. *J Histochem Cytochem,* 50**,** 1469-1474.

Osman, O. S., Selway, J. L., Harikumar, P. E., Stocker, C. J., Wargent, E. T., Cawthorne, M. A., Jassim, S. & Langlands, K. 2013. A novel method to assess collagen architecture in skin. *BMC Bioinformatics,* 14**,** 260.

Rawlins, J. M., Lam, W. L., Karoo, R. O., Naylor, I. L. & Sharpe, D. T. 2006. Quantifying collagen type in mature burn scars: a novel approach using histology and digital image analysis. *J Burn Care Res,* 27**,** 60-65.

Taher, L., Collette, N. M., Murugesh, D., Maxwell, E., Ovcharenko, I. & LOOTS, G. G. 2011. Global gene expression analysis of murine limb development. *PLoS One,* 6**,** e28358.

Van Zuijlen, P. P., Ruurda, J. J., Van Veen, H. A., Van Marle, J., Van Trier, A. J., Groenevelt, F., KREIS, R. W. & Middelkoop, E. 2003. Collagen morphology in human skin and scar tissue: no adaptations in response to mechanical loading at joints. *Burns,* 29**,** 423-31.

Varani, J., Dame, M. K., Rittie, L., Fligiel, S. E., Kang, S., Fisher, G. J. & Voorhees, J. J. 2006. Decreased collagen production in chronologically aged skin: roles of age-dependent alteration in fibroblast function and defective mechanical stimulation. *Am J Pathol,* 168**,** 1861-1868.

Varani, J., Warner, R. L., Gharaee-Kermani, M., Phan, S. H., Kang, S., Chung, J. H., Wang, Z. Q., Datta, S. C., Fisher, G. J. & Voorhees, J. J. 2000. Vitamin A antagonizes decreased cell growth and elevated collagen-degrading matrix metalloproteinases and stimulates collagen accumulation in naturally aged human skin. *J Invest Dermatol,* 114**,** 480-486.

Verhaegen, P. D., Marle, J. V., Kuehne, A., Schouten, H. J., Gaffney, E. A., Maini, P. K., Middelkoop, E. & Zuijlen, P. P. 2012. Collagen bundle morphometry in skin and scar tissue: a novel distance mapping method provides superior measurements compared to Fourier analysis. *J Microsc,* 245**,** 82-89.

Yano, K., Brown, L. F. & Detmar, M. 2001. Control of hair growth and follicle size by VEGF-mediated angiogenesis. *J Clin Invest,* 107**,** 409-17.

Yerpude, A. & Dubey, S. 2012. Colour image segmentation using K–Medoids Clustering. *Int. J. Computer Techology & Applications***,** 152-154.